Available online at www.sciencedirect.com
SCIENCE DIRECT
Polymer 47 (2006) 5843–5851
polymer
www.elsevier.com/locate/polymer

Studying the sol–gel transition of styrene–divinyl benzene crosslinking co-polymerization via excimer forming dye molecules

Ali Gelir [a], Demet Kaya Aktaş [a], Ioan Cianga [b,c], Luminita Cianga [b,c], Yusuf Yağcı [b], Yaşar Yılmaz [a,*]

[a] *Department of Physics, Istanbul Technical University, Maslak, 34469 Istanbul, Turkey*
[b] *Department of Chemistry, Istanbul Technical University, Maslak, 34469 Istanbul, Turkey*
[c] *''Petru Poni'' Institute of Macromolecular Chemistry, Grigore-Ghica Voda Alley, 41A, 700487 Iasi, Romania*

Received 24 March 2006; received in revised form 23 May 2006; accepted 9 June 2006
Available online 7 July 2006

Abstract

A novel method based on the steady state fluorescence technique was used to study the sol–gel transition in the free radical crosslinking reaction between styrene (St) and divinyl benzene (DVB) with 2,2′-azobisisobutyronitrile (AIBN) as initiator. *N*-(4-(pyrenyl methylene)-oxy-carbonyl phenyl)maleimide (Py-MI) was used as a fluorescence probe. The possible enchainment of Py-MI in alternating sequences occurred randomly in polymer clusters produced modifications in the fluorescence spectra, namely the shift at the higher wavelengths due to the excimer formation. The fluorescence spectra of Py-MI's excimers allowed both to monitor the sol–gel transition and to test the critical exponents as function of co-monomer's concentration. The gel fraction exponent β and the weight average degree of polymerization exponent γ agreed best with the static percolation values. Although this technique was applied for St–DVB co-polymerization, it may be generalized for the other monomers that are able to bind chemically to Py-MI monomer during the polymerization.

Keywords: Styrene; Excimer; Critical exponents

1. Introduction

Even though the sol–gel transition is not a phase transition in the thermodynamic sense, being a geometrical one, it behaves like a second order phase transition and constitutes a universal class by itself. An exact explanation for the sol–gel transition was first given by Flory and Stockmayer [1,2] by considering a special lattice, the so-called Bethe lattice, on which closed loops were ignored. Another approach to the problem is the lattice percolation model [3,4] where monomers are thought to occupy the sites of a periodic lattice. A bond between these lattice sites is formed randomly with probability p. For a certain bond concentration p_c, defined as the percolation threshold, the infinite cluster is formed in the thermodynamic limit. This cluster is called the gel. The polymeric system is in the sol state below the percolation threshold, p_c.

The predictions of these two theories about the critical exponents for the sol–gel transition are different from the universality point of view. For example, the weight average degree of polymerization DP_w (or average cluster size, S) and the gel fraction G, near the gel point, are defined as,

$$DP_w \propto (p_c - p)^{-\gamma}, \quad p \to p_c^- \tag{1}$$

$$G \propto (p - p_c)^{\beta}, \quad p \to p_c^+ \tag{2}$$

where the classical Flory–Stockmayer theory considers γ and β exponents, independent from the dimensionality of the space, $\gamma = \beta = 1$, while the percolation studies based on

* Corresponding author. Tel.: +90 212 285 3219; fax: +90 212 285 6386.
E-mail address: yyilmaz@itu.edu.tr (Y. Yılmaz).

0032-3861/$ - see front matter © 2006 Elsevier Ltd. All rights reserved.
doi:10.1016/j.polymer.2006.06.017

computer simulations give γ and β around 1.7 and 0.43, respectively, in three-dimension [3–8].

One would like to measure the values of the critical exponents with sufficient accuracy to determine their universality class and to verify that they indeed have the classical or the nonclassical values (for percolation, computed from series expansions and Monte Carlo studies as well as renormalization theory). But, due to the experimental difficulties and the different nature peculiar to the monomers of each kind no general procedure has been found, so far, for measuring the scaling behavior at the sol–gel transition, except for recent studies on the acrylamide polymerization [9]. Therefore, the results of classical and percolation theories have not been tested adequately for different kinds of polymer with real experiments.

Experimental techniques used for monitoring this transition must be very sensitive to the structural changes, and should not disturb the system mechanically. Preferably, one should have more than one quantity measured in the gelation experiments. Then, one can fix p_c from the best fit of data and use the same p_c for the other properties [3], if the gel point is not known accurately. If the gel point is known, in the experimentally reasonable limits, and if one has the chance of measuring more than one quantity in a single experiment, the reliability of exponents corresponding to measured physical quantities would increase greatly [3,9].

The fluorescence technique is particularly useful for elucidation of detailed structural aspects of the gels. This technique is based on the interpretation of the change in anisotropy, emission and/or excitation spectra, emission intensity, and viewing the lifetimes of injected aromatic molecules to monitor the change in their microenvironment [10–13]. Due to these special features, fluorescence spectroscopy has provided some of the most sensitive and selective methods of analysis for many compounds, typically in the fields of chemistry, biology and medicine [14,15].

The applications of fluorescence and phosphorescence spectroscopy as tools to study synthetic polymers have grown in number and scope over the last decades. Originally modeled after studies in biological sciences, these techniques were applied first to study hydrophobic synthetic polymers labeled with hydrophobic dyes [16]. Under these circumstances it could be argued with confidence that, a dye, grafted in small amounts along a macromolecule, would not modify substantially the solution or bulk properties of the material.

Fluorescence probes based on chromophores of different types are widely used for monitoring various processes and functions on a microscopic level [17,18]. Pyrene was the first aromatic hydrocarbon shown to exhibit excimer formation in solution [19]. Pyrene itself and its derivatives have earned reputation as versatile fluorescence probes for monitoring of photophysical and photochemical processes in various complex systems as micelles [20,21], polymers [22,23], gels [9,24–31,32] and biological structural units as vesicles and cells [33].

All parameters, which are sensitive to the change of the environment, might be used for this purpose. These compounds become chromophores of choice for this application because of the dependence of their vibrational structure on polarity, ability to form homo- and hetero-dimers in the excited state (excimers, exciplexes), and their long lifetimes in non-polar media (ca. 400 ns). Pyrene has been used successfully to probe the polarity of the medium during gelation [34,35] since the vibronic structure of the fluorescence spectrum is dependent on the environment [36].

By using tethered-pyrene compounds as probes of local organization and dynamics, characterization of oxidized gold, ITO and quartz substrates was reported [37]. The substituted pyrene derivatives were chosen because this chromophore exhibits ''polarity''-dependent changes in its linear optical response that are mediated by dipolar coupling between its S_1 and S_2 excited states and the immediate environment. The $S_2 \leftarrow S_0$ and $S_1 \leftarrow S_0$ electronic transitions in pyrene are polarized nominally perpendicular to one another, and the extent to which the local environment couples the coordinates spanned by b3g vibrational modes determines the observed perturbation to the chromophore linear response. For substituted pyrene compounds, the presence of constituent(s) serves to break the symmetry of the chromophore, but the extent to which the excited electronic states are coupled is still determined to a significant extent by the chromophore local environment. We have observed that the local environment of several substituted pyrene derivatives mediates the optical response by altering the extent of vibronic coupling between the S1 and S2 manifolds (vide infra) [9,38].

A recent work which used pyranine as a fluorescence probe [9] is of great importance in connection with the new experimental methods developed for determining the critical exponents at the sol–gel transition of acrylamide-*N*,*N*′-methylenebis (acrylamide) crosslinking polymerization. In this system the probe molecules bind to acrylamide polymer chains during polymerization, and fluoresce at different wavelengths when they bind to polymer chains. But, the probe used in this study [9] could not be generalized for other kind of polymers due to its incapability of binding to other kind of monomers.

In the present study we introduce a method for monitoring the sol–gel transition and measuring critical exponents around the critical point of St–DVB crosslinking co-polymerization. Here, Py-MI molecule was used as fluoroprobes. It binds chemically to St–DVB system like a monomer in an alternating sequence in parts of the polymer clusters, and produces modifications in the fluorescence spectra due to the excimer formation.

2. Experimental part

2.1. Materials

1-Pyrene aldehyde, $NaBH_4$ (Aldrich) were used as received. Maleic anhydride (Aldrich) was sublimated before use. Acetic anhydride (Merck) and *p*-aminobenzoic acid were used without further purification. Thionyl chloride and St (Fluka) were distilled just before use. The solvent, tetrahydrofuran (THF) (Merck) was distilled twice over sodium. The initiator AIBN (Merck), was recrystallized twice from methanol. DVB (Merck) was shaken with 5% NaOH, washed with water, dried with anhydrous $CaCl_2$, and finally distilled

under reduced pressure. Purity was checked by gas chromatography. Various batches of DVB solution were used. Batch analyses ranged between 50 and 60% DVB isomers (*m*-DVB: *p*-DVB ratio 3.2–3.25:1), the rest being ethylstyrene.

2.2. Synthesis of the intermediates and maleimide monomer

2.2.1. Synthesis of 1-pyrenyl methanol

This intermediate was synthesized by a reduction reaction starting from 1-pyrene aldehyde as was reported [39].

^{1}H NMR ($CDCl_3$) (δ, ppm): 8.27–7.93 (m, 9H, pyrenyl), 5.29 (s, 2H, CH_2), 2.21 (s, broad, 1H, OH).

IR (cm^{-1}): 3200–3600 (broad) (OH), 1005 (C–OH).

2.2.2. Synthesis of 4-maleimidobenzoic acid

This was synthesized by the condensation reaction of maleic anhydride with *p*-aminobenzoic acid followed by cyclodehydration using acetic anhydride and sodium acetate according to a literature procedure [40].

Yield 85%; mp. 234 °C (mp. (lit. [37]) 244 °C); IR (cm^{-1}): 3460–3200 (COOH); 3105-3100 (=CH); 1720 (O=CNC=O); 1610 (C=C); 1217 (C–O); 820 (phenyl); 720 (*cis* CH=CH).

2.2.3. Synthesis of 4-maleimidobenzoic acid chloride

This was synthesized according to a literature procedure [40].

Yield 73%; mp. 157–158 °C (mp. (lit. [37])168–169 °C); IR (cm^{-1}): 1770 (COCl); 1715 (O=CNC=O); 1600 (C=C); 700 (*cis* CH=CH).

2.2.4. Synthesis of N-(4-(pyrenyl methylene)-oxycarbonyl phenyl)maleimide (Py-MI)

Pyrene-maleimide (Py-MI) monomer was synthesized starting from 4-maleimidobenzoic acid chloride and 1-pyrenyl methanol by a Schotten–Bauman type reaction, using a procedure similar to thienyl-containing maleimide [41].

Yield 87%; mp. (DSC) = 191–192 °C.

^{1}H NMR (DMSO-d_6) (ppm): 8.5–8.03 (m, 11H, pyrenyl-H + Ar-H ortho to CO); 7.54–7.45 (d, 2H, Ar-H, ortho to N), 7.22–7.18 (s, 2H, double bond maleimide), 6.14-6.04 (s, 2H, CH_2).

2.2.5. Synthesis of St–DVB crosslinked gels in the presence of Py-MI probes

Gels were prepared by using various amounts of St, Py-MI, DVB and AIBN, by dissolving them in THF (solution polymerization, see Sample 1 in Table 1) or in the bulk form (bulk polymerization, i.e., no solvent was added to the samples where St acts as solvent for Py-MI, DVB and AIBN, see Samples 2–4 in Table 1). All samples were deoxygenated by bubbling nitrogen for 10 min, just before the polymerization process. Having prepared the pre-polymer samples each shown in Table 1, they were kept at 70 °C in sample holder of the fluorescence spectrometer, and fluorescence and light scattering experiments (turbidity measurements) were performed during the polymerization.

Table 1
Chemical compositions of the samples used for sol–gel transition and the estimated values of γ and β exponents for the ratio C^+/C^-[a]

Sample	Reaction conditions				$t_{c(min)} \pm 0.1$	C^+/C^-	γ	β
	Styrene (mmol)	Py-MI (μmol)	DVB (μmol)	THF (ml)				
1	8.7	2.0	0.14	3.0	41	2.7	0.6	0.52
						3.5		0.52
						4.3		0.52
						10		0.52
						1.0		1.00
2	17.4	8.1	0.28	0	20.3	2.7	1.8	0.46
						3.5		0.46
						4.3		0.46
						10		0.40
						1.0		0.90
3	13.1	8.1	0.21	0	25.9	2.7	1.8	0.47
						3.5		0.47
						4.3		0.50
						10		0.43
						1.0		0.90
4	8.7	11.6	0.14	0	73	2.7	0.6	0.43
						3.5		0.43
						4.3		0.38
						10		0.35
						1.0		1.00
5	8.7	21.0	0.14	0	9.3	2.7	1.8	0.30
						3.5		0.30
						4.3		0.25
						10		0.15
						1.0		0.80
6	8.7	271.0	0.14	0	38	2.7	1.8	0.54
						3.5		0.54
						4.3		0.36
						10		0.30
						1.0		1.05

[a] All experiments were performed at 70 ± 2 °C.

2.3. Measurements

The fluorescence and scattered light intensity measurements were carried out using the Model LS-50 spectrometer of Perkin–Elmer, equipped with a temperature controller. The concentrations of the chromophore, Py-MI, used in pre-polymer solutions were in trace amounts as seen from Table 1. All measurements were made at 90° position and slit widths were kept at 5 mm. Py-MI was excited at 345 nm during steady state fluorescence experiments (SSF), and variation in the scattered light at 345 nm, fluorescence spectra and emission intensity of the Py-MI were monitored simultaneously as a function of gelation time.

3. Results and discussion

3.1. Fluorescence characteristics and binding process of Py-MI to St monomers

In the first part of this work, fluorescence characteristics of Py-MI monomer and the binding process of Py-MI to St were studied.

Fig. 1 shows the molecular structure, excitation and emission spectra of Py-MI dissolved in THF at different

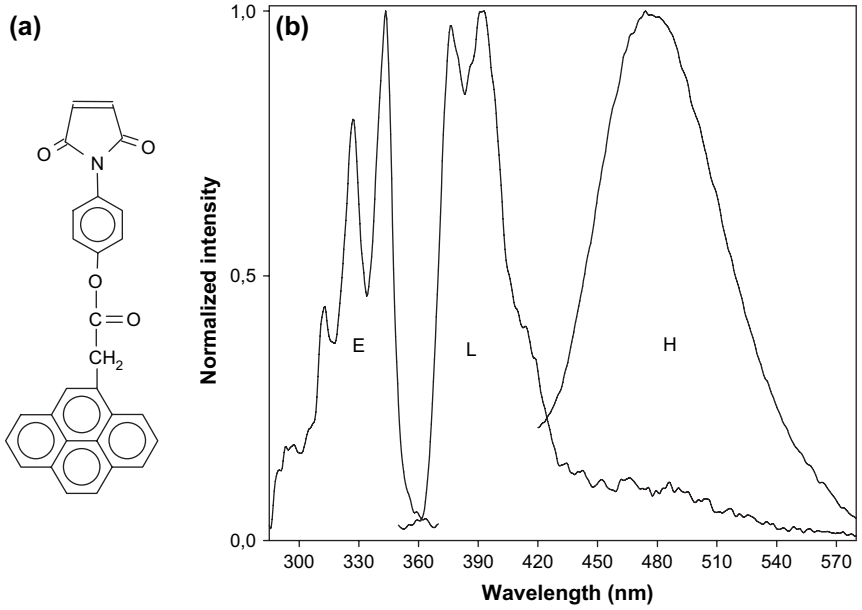

Fig. 1. Molecular structure (a) and excitation/emission spectra of Py-MI solution in tetrahydrofuran (THF) (b). E: the excitation spectrum of Py-MI; L: the emission spectrum of Py-MI at low concentration; H: the emission spectrum of Py-MI at high concentration.

concentrations. In the case of dilute solutions, only the peak around 390 nm is observed. This peak corresponds to Py monomer spectra [25,42–47]. For high concentration of Py-MI an excimer peak appears around 480 nm [42–47].

To examine the polymerization process of St with Py-MI with varying initial concentrations of St and Py-MI molecules, both fluorescence and NMR measurement were performed on these samples after the polymerization processes were completed. NMR measurements showed that if the initial ratio of [Py-MI]/[St] in the pre-polymerization samples is close to unity, the percentage of the St and Py-MI molecules on the resulting polymer chains are close to each other. But, when this ratio is decreased below unity, the percentage of the Py-MI molecules on the polymer chains decreases.

Fluorescence spectra for three linear polymer samples dissolved in THF are compared in Fig. 2. As the initial ratio of [Py-MI]/[St] is decreased the maximum intensity corresponding to the excimer peak decreases, indicating that the number of Py-MI pairs on the polymer chains leading to the excimer formation decreases. The fact that the peak corresponding to the monomer emission (around 390 nm peak) was also observed in Fig. 2 together with the excimer emission (480 nm peak) indicates that the Py-MI monomers both constitute some alternating parts of sequences and distributed randomly far-off the others along the polymer chains. The excimer spectra come from the alternating parts (paired Py's), and monomer spectra come from the randomly distributed Py-MI monomers (unpaired Py's). Fig. 2 also shows that the probability of forming the alternating sequence, as observed by NMR measurements, increases as the initial ratio of [Py-MI]/[St] is increased.

These observations clearly indicate that Py-MI could be used as a probe such that it is able to make excimers in alternating sequences. These alternating sequences should distribute over the gelling system as parts of the polymer clusters. In the following section, we will show that these excimer forming fragments monitor the weight average cluster size and gel fraction around the sol–gel transition of the system under consideration.

3.2. Gelation experiments

In this part of the work, St–DVB co-polymerization (gelation) experiments were performed with varying amounts of Py-MI as seen in Table 1.

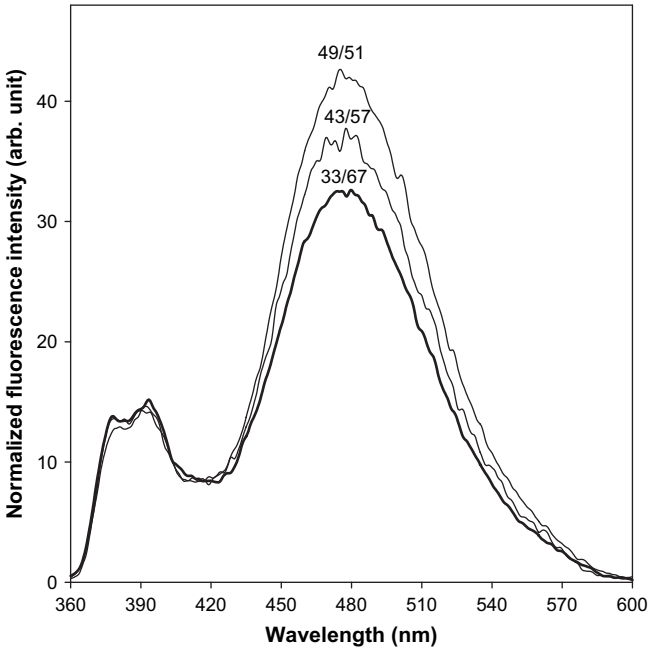

Fig. 2. Fluorescence spectra from the linear polymer samples, including alternating Py-M and St contents. The numbers on each curve indicates [Py-M]/[St] ratio on the polymer chains calculated by NMR measurements.

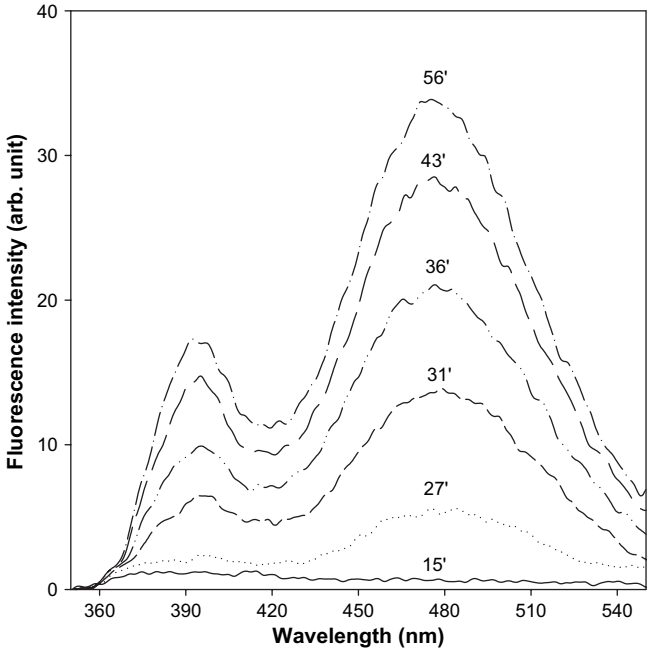

Fig. 3. Fluorescence spectra registered during gelation of Py-MI with St and DVB. Numbers on each curve indicate the corresponding reaction times.

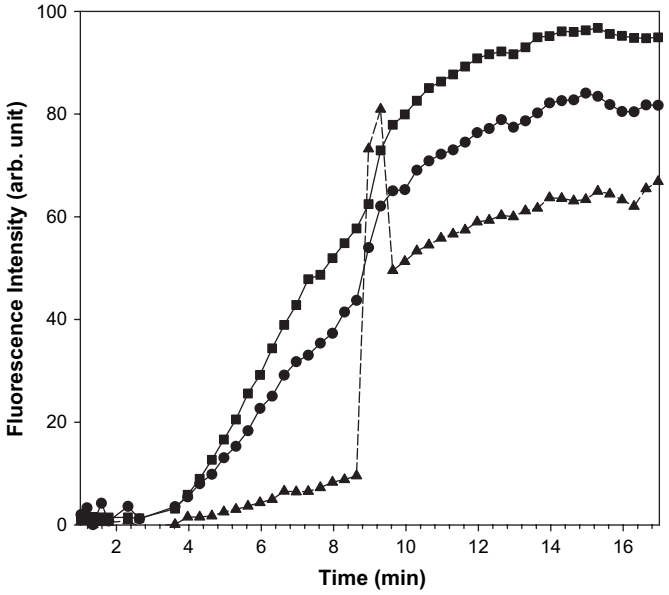

Fig. 4. Typical fluorescence intensities of the Py-M during the gelation process of St/Py-MI/DVB crosslinking co-polymerization. Squares, circles and triangles represent the maximum intensities corresponding to excimer, monomer peaks, and scattered intensity, respectively. The solid lines are given to guide the eye.

Fig. 3 shows an example for the variation of the fluorescence spectra registered during gelation of St and DVB in the presence of Py-MI. As seen from Fig. 3 upon the initiation of the polymerization a new peak first appears around 480 nm due to excimer formation of the Py's on the MI groups, and the intensity of this peak increases (more rapidly compared to the increase in the monomer emission intensity) during the gelation process. Increase in the intensities of both excimer and Py-MI monomer peaks during the polymerization is due to both the increase in the excimer formation during polymerization and the increase in the local viscosity around the Py-MI molecules both free in the sample cell or bonded to the polymer chains so as to be far-off the other Py-MI molecules.

Fig. 4 shows typical changes in the excimer and monomer fluorescence intensities, and scattered intensity of excited light at 90°, as a function of the gelation time of the St–DVB crosslinking co-polymerization. When a critical time t_c is reached the samples start to form bulky materials insoluble in any solvent; the gel. At the end of the reaction time the samples turn to the glassy or rubber-like gel samples depending on the initial composition of monomers. The sample including THF content (see Sample 1 in Table 1) turns to the rubber-like gel sample, and the others which do not include THF (see Samples 1–3) to the glassy materials.

Before discussing the position of the gel point, p_c, here we would like to argue that the excimer intensity is directly proportional to the average cluster size of the polymers below the gel point, and the gel fraction (when the intensity from the small clusters is subtracted from the total intensity) above the gel point. This proportionality can easily be proven by using the similar arguments as discussed previously [9], using a lattice model [3,4] where monomers occupy the sites of an imaginary periodic lattice.

The probability, w_s that the cluster (the group of the monomers that are connected to each other) to which an arbitrary occupied site (monomer) belongs contains exactly s sites (s number of monomers) is [3,4],

$$w_s = \frac{n_s \cdot s}{\sum_s n_s \cdot s} \tag{3}$$

where n_s is the number of *s-cluster* (number of clusters each including s monomers) per lattice site (or monomer). Thus, the average cluster size, S (or weight average degree of polymerization, DP_w, in polymer language) is calculated by the following relation [3–6].

$$S = \sum_s w_s \cdot s = \frac{\sum n_s \cdot s^2}{\sum n_s \cdot s} \tag{4}$$

Now, let N_p be the number of Py-MI molecules in the sample, N_s be the number of St molecules, and N_m the total number of the other molecules (DVB, AIBN, THF) except for Py-MI and St. Thus, the total lattice site, $N = N_p + N_s + N_m$.

The probability, P_p that arbitrary two Py-MI molecules form an alternating sequence with an St molecule can be calculated as

$$P_p = \frac{1}{3}\left(\frac{N_p}{N}\right)^2\left(\frac{N_s}{N}\right) \tag{5}$$

This simple alternating part, (Py-MI)-St-(Py-MI), which will be called a "pyrene-pair", is the main unit of the excimer forming parts of the polymer chains,

The probability, P_y, that a pyrene-pair chosen randomly belongs to any cluster of size s (the *s-cluster* or a macromolecule including s monomers) will be the product of w_s and P_p.

$$P_y = P_p \cdot w_s = \frac{P_p \cdot n_s \cdot s}{\sum n_s \cdot s} \tag{6}$$

Thus, $P_y \cdot s$ gives the total number of pyrene-pairs in an *s-cluster*. The total excimer fluorescence intensity, I_{exc}, which is proportional to the total number of pyrene-pairs distributed randomly infinite clusters of varying size, can be calculated as a summation over all *s-clusters*,

$$I_{exc} \sim \sum_s P_y \cdot s = \sum_s \frac{P_p \cdot n_s \cdot s}{\sum n_s \cdot s} \cdot s = \frac{\sum P_p \cdot n_s \cdot s^2}{\sum n_s \cdot s} \tag{7}$$

Since the concentrations of the components are kept fixed for each sample, P_p is a constant, thus can be taken out of the summation in Eq. (7),

$$I_{exc} \sim P_p \frac{\sum n_s \cdot s^2}{\sum n_s \cdot s} = \frac{1}{3}\left(\frac{N_p}{N}\right)^2 \left(\frac{N_s}{N}\right) S \tag{8}$$

The last expression indicates that the total normalized excimer fluorescent intensity, I_{exc}, is proportional to the average cluster size S (or the weight average degree of polymerization DP_w).

In the above derivation we assumed that the variation in the viscosity of the samples, near the gelation threshold, does not affect the excimer intensity considerably. Once a pyranine binds to a polymer strand it is not so much free to move freely in the sample, especially above and below – but close to – the gel point. But, the main contribution to the monomer intensity due to the change in the sample viscosity comes from the free pyranines, because they are totally free to interact and be quenched by the ''sol'' molecules.

Now, we would like to argue the connection of the reaction time with the bond formation probability, p, given by the relation in Ref. [31], given by

$$p = SC\frac{v_0}{V} \equiv \frac{v_0}{V} \tag{9}$$

Here, C is the total number of clusters of average size S, $v_0 = V/N$ is the volume occupied by a single monomer, and N is the total number of monomers. The average cluster size, S of the clusters obeys the differential equation [31]

$$\frac{dS(t)}{dt} = k(N - CS) \tag{10}$$

over a sufficiently short time interval. Here the time dependence of the reaction rate constant k due to the change in the viscosity, and of C due to the gradual dissolution and termination of the initiators can be neglected. Thus, for relatively short time intervals, we get a linear growth law,

$$S(t) - S(t_0) = [S_\infty - S(t_0)]kC(t - t_0) \tag{11}$$

where $S_\infty = N/C$, and t_0 is an arbitrary starting point. Defining t_c as the time at which the percolation threshold p_c is reached, and using Eq. (9), we have, for sufficiently small $|t - t_c|$,

$$|t - t_c| = \frac{1}{kC}\frac{|p - p_c|}{1 - p_c} \propto |p - p_c| \tag{12}$$

The last expression shows that in the critical region, i.e., around the critical point, $|p - p_c|$ is linearly proportional to the $|t - t_c|$ [9,26,31,48]. Therefore, below the gel point, i.e., for $t < t_c$, the excimer fluorescence intensity, I_{exc}, measures the average cluster size, S (or weight average degree of polymers DP_w). Let I_{ct} be the total excimer fluorescence intensity of finite clusters distributed through the infinite network. Thus, $I_{exc} - I_{ct}$ measures solely the gel fraction G, that is, the fraction of the monomers that belong to the macroscopic network [9]. Here, I_{exc} is the total excimer fluorescence intensity both from the ''infinite cluster'' and finite clusters distributed through this ''infinite cluster''. In summary, we have the following relations,

$$I_{exc} \propto S = C^+(t_c - t)^{-\gamma}, \quad t \to t_c^- \tag{13a}$$

$$I_{ct} \propto S = C^-(t_c - t)^{-\gamma'}, \quad t \to t_c^+ \tag{13b}$$

$$I_{exc} - I_{ct} \propto G = B(t - t_c)^{\beta}, \quad t \to t_c^+ \tag{14}$$

where C^+, C^- and B are the critical amplitudes.

One can also measure the degree of polymerization or average size of finite clusters above the gel point in the sol coexisting with gel: then the critical behavior can be described by another critical exponent γ', which has the same value with γ [3–6,9]. But, the critical amplitudes for the average cluster size defined below (C^+ in Eq. (13a)) and above (C^- in Eq. (13b)) the gel point are different, and there exists a universal value for the ratio C^+/C^-. This ratio is different for mean-field versus percolation as discussed in detail by Aharony [7] and Stauffer [3]. The estimated values for C^+/C^- are given in Ref. [7].

To determine the intensity I_{ct} in Eqs. (13b) and (14), we first chose the part of the intensity–time curves up to the gel points, then the mirror symmetry I_{ms} of this part with respect to the axis perpendicular to time axis at the gel point were multiplied by the ratio C^-/C^+, so that $I_{ct}=(C^-)/(C^+)I_{ms}$ [13]. Thus, I_{ct} measures solely the intensity from the finite cluster above the gel point, and $I_{exc}-I_{ct}$ measures the intensity from the gel fraction. This process is clarified explicitly in Ref. [9].

Now, we would like to introduce our methods for determining the critical time (or gelation time), t_c. Naively speaking, one might guess that by taking the derivatives of the intensity, $I_{exc}(t)$ curves, as was done in Fig. 5, the critical point may be obtained from the maxima of these curves. It was found that [26] the t_c obtained from the best scaling fits, were consistently smaller than the times t_m at which the maxima of the dI_{exc}/dt curves appear. Finite size scaling [4] predicts that the difference $t_m - t_c$ (t_c is the critical time) vanishes as $L^{-1/\nu}$, where L is the size of the system as measured in units of the lattice spacing, and ν is the correlation length exponent. Moreover, the width of the dI_{exc}/dt curve (which argued that behaves like the dP_∞/dp curve, where P is the strength of the infinite

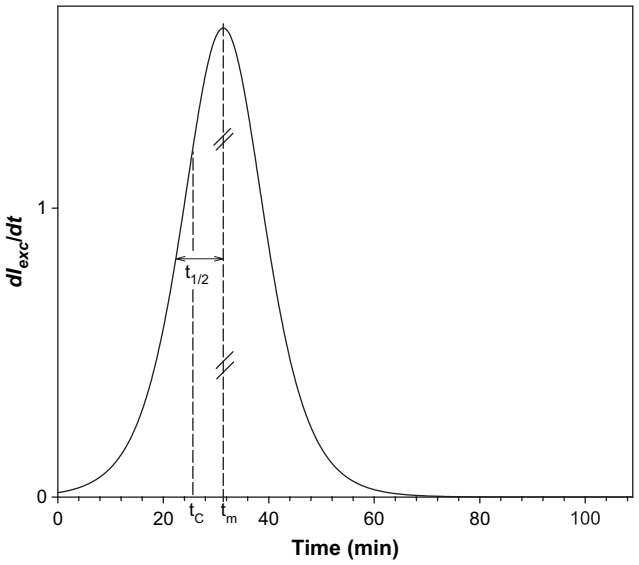

Fig. 5. The first derivative dI_{exc}/dt of a typical sample, against the reaction time t. The time corresponding the maximum is consistently greater than the critical time t_c.

network), measured at half height or any other conveniently chosen point, should be proportional to t_c-t_m and scale with the same power of L [4]. In agreement with finite size scaling, the ratio of $t_m - t_c$ to $t_{1/2}$, the half width at half maximum of the dI_{exc}/dt curves, was found to be a constant,

$$\frac{t_m - t_c}{t_{1/2}} = 0.248 \pm 0.005 \tag{15}$$

over the whole range of experiments, with varying Py-MI concentrations. Therefore, the real critical point is somewhat before the maxima of the derivative of the fluorescence intensity as shown in Fig. 5. It is observed that at the same t_c the scattered light intensity measured during the gelation experiments as demonstrated in Fig. 4 passes through a maximum.

We performed both solution polymerization (in which some amount of THF was added as solvent) and bulk polymerizations (i.e., the samples in which no solvent was added) as in Table 1. Fig. 6 represents typical excimer fluorescence intensity–time curves for varying St, Py-MI and THF contents. It is observed that when the Py-MI concentration is chosen high enough, a stepwise change occurs (as shown in plot (d) of Fig. 6) in the intensity just at the critical point t_c. It was also observed that above a certain Py-MI concentration the samples became highly turbid (Sample 4 in Table 1) not just at the critical point but also below it.

Using Eqs. (13) and (14), and the values for critical t_c we calculated γ and β exponents as function of St/Py-MI concentration ratio, DVB concentration and initiator concentration. Fig. 7 represents the log–log plots of some typical intensity–time data above and below the gel point, where the slopes of the straight lines, close to the gel points, give β and γ exponents, respectively.

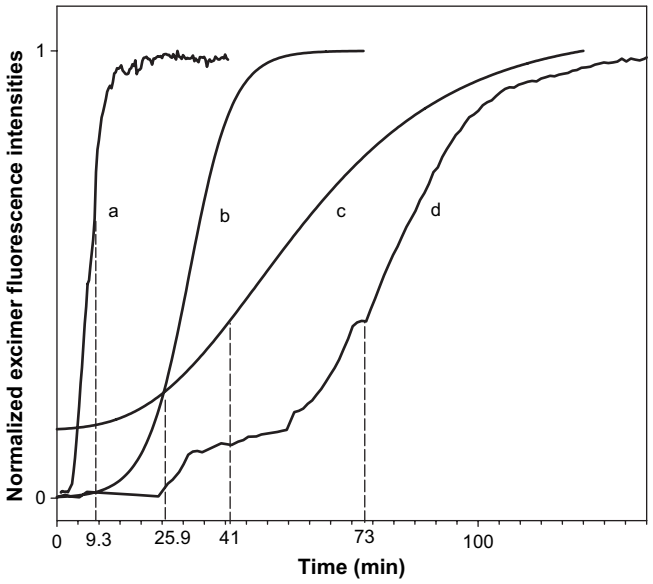

Fig. 6. Excimer fluorescence intensity as a function of reaction time for different St, Py-MI and THF content; (a) for Sample 5, (b) for Sample 3, (c) for Sample 1, (d) for Sample 4 given in Table 1. The dashed lines indicate the corresponding critical times.

The composition of the ingredients C^-/C^+ dependence of the exponents are summarized in Table 1. As seen from the table for the samples including high Py-M and THF contents, the γ exponents deviate from the percolation results. This is due to a considerable change in opacity as the critical point is reached, which results in a change in the intensities entering the gel, and thus in emission.

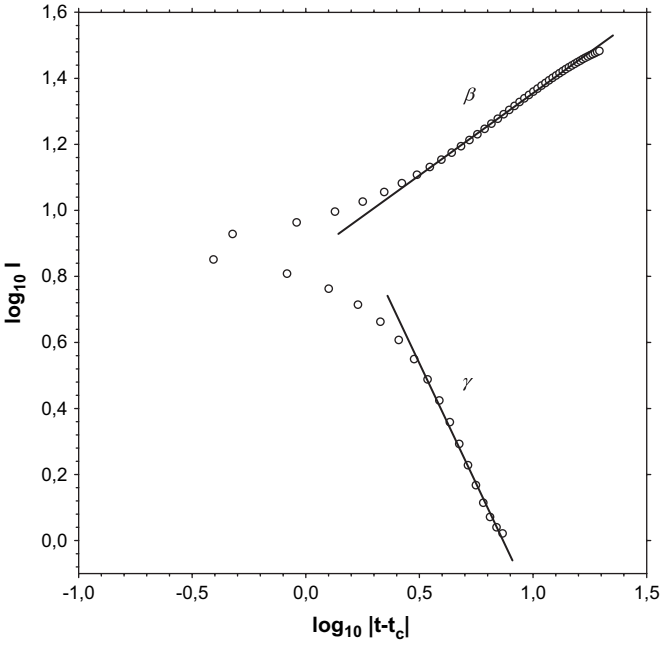

Fig. 7. A typical double logarithmic plot of the intensities versus $|t - t_c|$. The γ and β exponents were determined from the slope of the straight lines, near the gel points for $t < t_c$ and $t > t_c$, respectively.

4. Conclusion

The application of an intrinsic fluoroprobe, Py-MI, is illustrated for *in situ* monitoring of free radical crosslinking copolymerization of St–DVB. The probe molecules fluoresce at different wavelengths when they are incorporated into growing polymer chains so as to form excimer. The excimer fluorescence intensity of the pyrene-pairs is therefore a measure of the degree of polymerization and gel fraction near the sol–gel transition threshold. We are, thus, able to measure polymerization kinetics directly without disturbing the system mechanically, and to test the universality of the sol–gel transition as a function of the co-monomer's concentration.

As seen from Table 1, the exponents (especially γ exponent) deviate remarkably from both the classical and percolation results for Samples 1 and 4, but the exponents for the other samples agree best with the percolation results ($\beta = 0.45$, $\gamma = 1.8$), where β is independent of the values of C^+/C^- except for its classical value $C^+/C^- = 1$. For $C^+/C^- = 1$, the values of the β exponents for any composition of the co-monomers (St and DVB), solvent (THF) and probe (Py-MI) agree with the classical results ($\beta = 1$) as previously observed for the sol–gel transition of acrylamide for relatively low concentrations [9].

The nonuniversal behavior for the sample including considerable amount of solvent (THF) may be due to the fact that we are extremely far away from the critical region for these experimental conditions. It can be easily shown that the THF volume fraction V_{THF} is simply proportional to the internal lower cutoff, l (the expected minimum length of a strand between two branching points on the incipient percolating network) $l \propto V_{THF}$ (see Ref. [26]). For relatively higher THF contents, with correspondingly larger l, the values of β and γ start to deviate markedly from their expected values. Clearly, for larger $l = aN$, (where a is the average bond length and N is the number of monomer) finite size effects become more pronounced, driving the system further away from the asymptotic critical region. An experimental system with intermediate N will exhibit a crossover between mean-field behavior far from the gel point and critical behavior, close to the percolation threshold, in a manner similar to other continuous phase transitions [9]. For large N the critical region in which the exponents are calculated is quite small. Thus, the entire range of experimentally accessible $|p - p_c|$ will be in the mean-field class and modeled by the Flory–Stockmayer theory [1,2]. The nonuniversal behavior for extremely low concentrations may be due to the fact that we are extremely far away from the critical region for these experimental conditions.

As seen from Table 1, the exponents deviate markedly from their expected values for the sample including relatively higher Py-MI content. As the Py-MI concentration is increased the local heterogeneity increases since Py-MI and St molecules prefer binding alternatively and form Py-MI rich regions, and thus the high contrast for these samples. Therefore, the deviation in both γ and β exponents for these samples may be due to the loss of emission intensity as the turbidity increases.

If the sample has a considerable opacity, the change in the fluorescence intensity cannot be interpreted as being due solely to the excimer intensity. Another effect on the fluorescence intensity is the change in the opacity through polymerization. Therefore, the emission intensity at 390 nm must be corrected by taking into account the scattered light to find the real change in the fluorescence intensity for samples having considerable opacity. Using the measured emission intensity $I_{exc}(t)$ at 390 nm, and scattered light intensity $S(t)$, the corrected fluorescence intensity, $I_{exc}^{corr}(t)$, can be calculated as $I_{exc}^{corr}(t) = k \cdot I(t) \cdot S(t)$. This relation can be obtained by normalizing the measured fluorescence intensity $I_{exc}(t)$ with a function $f(t)$, as $I_{exc}(t)/f(t)$, so that $f(t)$ keeps the scattered intensity fixed during the polymerization, i.e., $S(t) \cdot f(t) = 1/k$, where k is a constant number. Of course, the sample turbidity is controlled by the total scattering cross section (i.e., the differential scattering cross section integrated over all angles, $S(\theta)$), and not just by cross section at 90°, $S(90°)$, which is proportional to the differential scattering cross section at $\theta = 90°$. Therefore, we believe that if $S(\theta)$ could be measured simultaneously with fluorescence measurements it may be possible to calculate the critical exponents in opaque interval.

Although this technique could be seen as special to the St–DVB co-polymerization, this method may be generalized for other monomers that are able to bind chemically to Py-MI monomer during the polymerization. Or, the aromatic molecules having acrylate group/groups could be used as probe molecules for many kinds of monomers. In this way there will be two possibilities during the polymerization: either the probe molecules will fluoresce at different wavelength when they bonded to the polymeric systems, or they will come close during the course of the polymerization and form excimer. Monitoring new fluorescence band could give the chance of monitoring the polymerization without disturbing the sample.

Acknowledgements

Y. Yılmaz has been supported by the Turkish Academy of Sciences (TUBA) in the framework of the Young Scientist Award Program (EA-TÜBA-GEBİP/2001-1-1). I. Cianga and L. Cianga thank TUBITAK for the financial support that was given through postdoctoral fellowships.

References

[1] Flory PJ. J Am Chem Soc 1941;63:3083 [see also 3091 and 3096].
[2] Stockmayer W. J Chem Phys 1943;11:45. 1944;12:125.
[3] Stauffer D, Coniglio A, Adam M. Adv Polym Sci 1982;44:193.
[4] Stauffer D, Aharony A. Introduction to percolation theory. 2nd ed. London: Taylor and Francis; 1994.
[5] Sahimi M. Application of percolation theory. London: Taylor and Francis; 1994.
[6] de Gennes PG. Scaling concepts in polymer physics. Ithaca, NY: Cornell University Press; 1988. p. 54.
[7] Aharony A. Phys Rev B 1980;22:400.
[8] Colby RH, Rubinstein M. Phys Rev E 1993;48:3712.
[9] Kaya D, Pekcan Ö, Yılmaz Y. Phys Rev E 2004;69:016117.

[10] Barrow GM. Introduction to molecular spectroscopy. New York: McGraw-Hill; 1962.
[11] Birks JB. Photophysics of aromatic molecules. London: Wiley; 1965.
[12] Herculus DM, editor. Fluorescence and phosphorescence analysis. New York: Wiley; 1965.
[13] Galanin MD. Luminescence of molecules and crystals. Cambridge: Cambridge International Science; 1995.
[14] Rettig W, Strehmel B, Schrader S, Seifert H, editors. Applied fluorescence in chemistry, biology and medicine. New York: Springer; 1999.
[15] Guilbault WE. Practical fluorescence theory, methods, and techniques. New York: Marcel Dekker; 1973.
[16] Winnik MA, editor. Photophysical and photochemical tools in polymer science. Holland: D. Reidel; 1986.
[17] Mayer A, Neuenhofer S. Angew Chem Int Ed 1994;33:1044.
[18] Rettig W, Lapouyarde R. In: Lakowicz JR, editor. Topics in fluorescence spectroscopy probe design and chemical sensing, vol. 4. New York: Plenum Press; 1994. p. 109.
[19] Forster T, Kasper KZ. Electrochemistry 1955;59:976.
[20] Winnik FM, Regismond STA. Colloid Surf A: Physicochem Eng Asp 1996;1:118.
[21] Capek I. Adv Colloid Interface Sci 2002;97:91.
[22] Winnik FM. Chem Rev 1993;93:587.
[23] Morawetz HJ. Polym Sci A: Polym Chem 1999;37:1725.
[24] Pekcan Ö, Yılmaz Y, Okay O. Chem Phys Lett 1994;229:537.
[25] Pekcan Ö, Yılmaz Y, Okay O. Polymer 1997;38:1693.
[26] Yılmaz Y, Erzan A, Pekcan Ö. Phys Rev E 1998;58:7487.
[27] Okay O, Kaya D, Pekcan Ö. Polymer 1999;40:6179.
[28] Oya T, Enoki T, Grosberg AY, Masamune S, Sakiyama T, Takeoka Y, et al. Science 1999;286:1543.
[29] Yılmaz Y, Yagcı Y, Pekcan Ö. J Macromol Sci, Pure Appl Chem 2001; A38(7):741.
[30] Yılmaz Y. Phys Rev E 2002;66:05801.
[31] Yılmaz Y, Erzan A, Pekcan Ö. Eur Phys J E 2002;9:135.
[32] Yılmaz Y, Kaya D, Pekcan Ö. Eur Phys J E 2004;15:19.
[33] Duportail G, Lianos P. Vesicles. In: Rosoff M, editor. New York: Marcel Dekker; 1996. p. 295 [chapter 8].
[34] Kaufman VR, Avnir D. Langmuir 1986;2:217.
[35] Zink JI, Dunn BS. J Ceram Soc Jpn 1991;99:878.
[36] Dong DC, Winnik MK. Can J Chem 1985;62:2560.
[37] Kelepouris L, Krysinski P, Blanchard GJ. J Phys Chem B 2003;107:4100.
[38] Yılmaz Y, Alemdar A. Appl Clay Sci 2005;30:154.
[39] Erdogan M, Hepuzer Y, Cianga I, Yagci Y, Pekcan O. J Phys Chem A 2003;107:8386.
[40] Cianga L, Olaru N. Design Monom Polym 2000;3:209.
[41] Yilmaz F, Cianga L, Guner Y, Toppare L, Yagci Y. Polymer 2004;45:5765.
[42] Thomas A, Polarz S, Antonietti M. J Phys Chem B 2003;107:5081–7.
[43] Chen Wei, Durning Christopher J, Turro Nicholas J. Macromolecules 1999;32:4151–3.
[44] Turro Nicholas J, Kuo Ping-Lin. Langmuir 1986;2:438–42.
[45] Turro Nicholas J, Kuo Ping-Lin. J Phys Chem 1987;91:3321–5.
[46] Principi Tania, Winnik Francoise M. Macromolecules 2000;33:3244–9.
[47] Chandar Prem, Somasundaran P, Turro Nicholas J, Waterman Kenneth C. Langmuir 1987;3:298–300.
[48] Tuzel E, Özmetin M, Yılmaz Y, Pekcan Ö. Eur Polym J 2000;36:727.